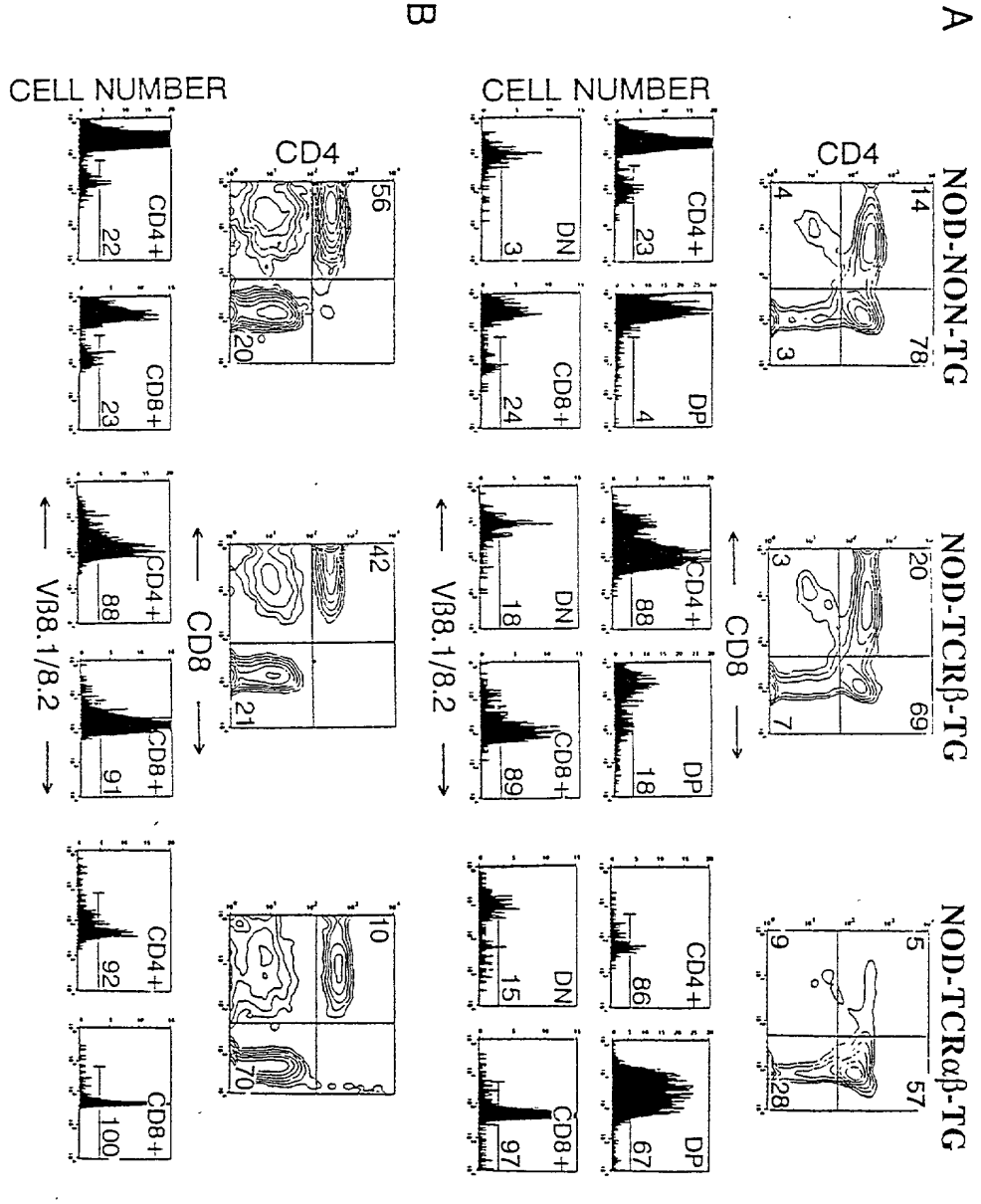

Fig. 1. TCRαβ Transgene Expression in 8.3-NOD Mice. CD4/CD8/Vβ8.1/8.2 profiles of thymocytes **(A)** and lymph node cells **(B)** from non-transgenic-, 8.3 TCRβ-transgenic-, and 8.3NOD mice. DP, double-positive; DN, double-negative.

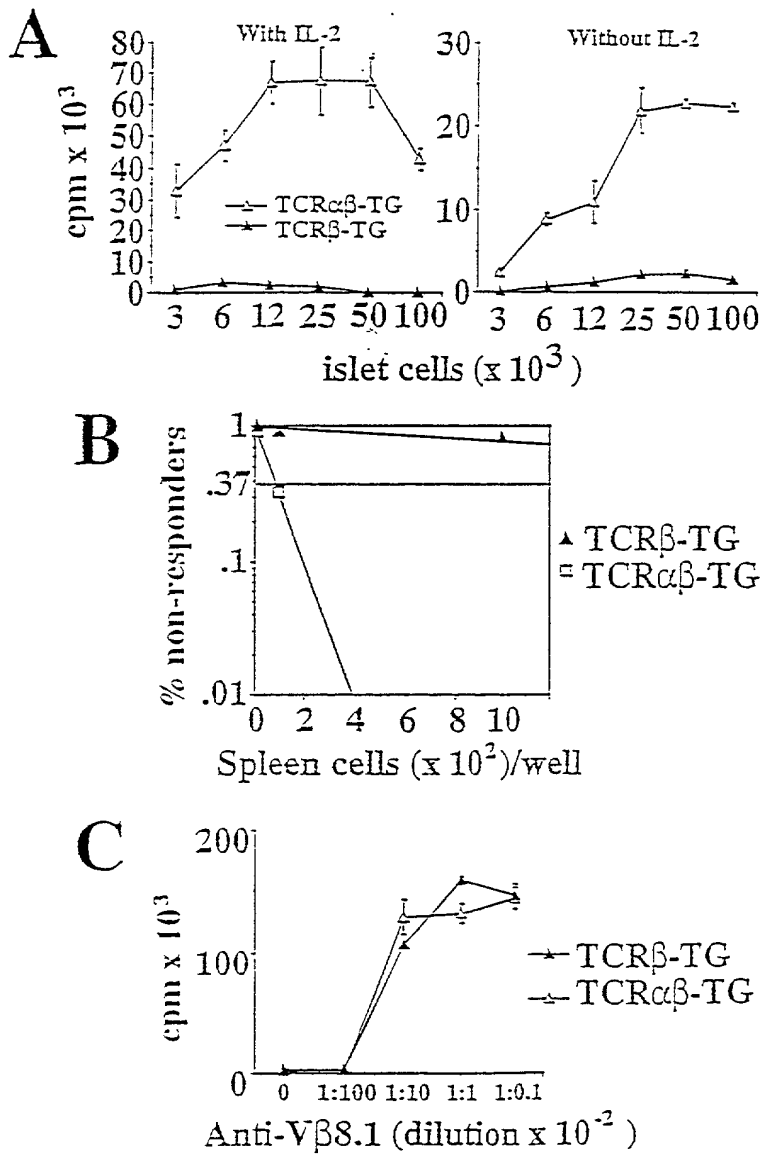

Fig. 2. Beta Cell-Specific CD8+ T-Cells in 8.3-NOD Mice. (A) Proliferation of splenic CD8+ T-cells to islet cells. (B) Peripheral frequency of beta cell-reactive CD8+ T-cells. (C) General proliferative activity of splenic CD8+ T-cells.

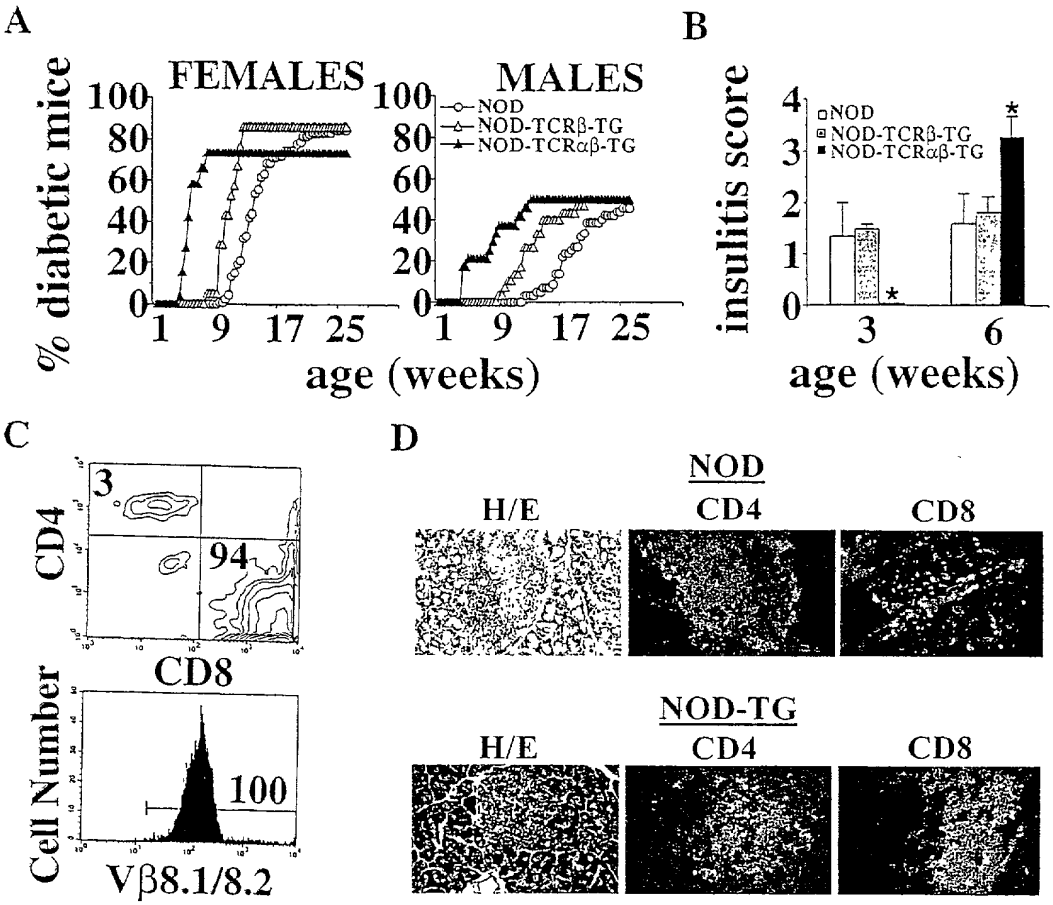

Fig. 3. 8.3-TCRαβ-Transgene Expression and Diabetogenesis. (A) Incidence of IDDM. (B) Progression of insulitis. *, $p<0.0001$ (χ^2). (C) Flow cytometry profile of islet-derived T-cells from diabetic 8.3-NOD mice. (D) Phenotype of islet-infiltrating T-cells in 8.3-NOD vs. non-transgenic NOD mice.

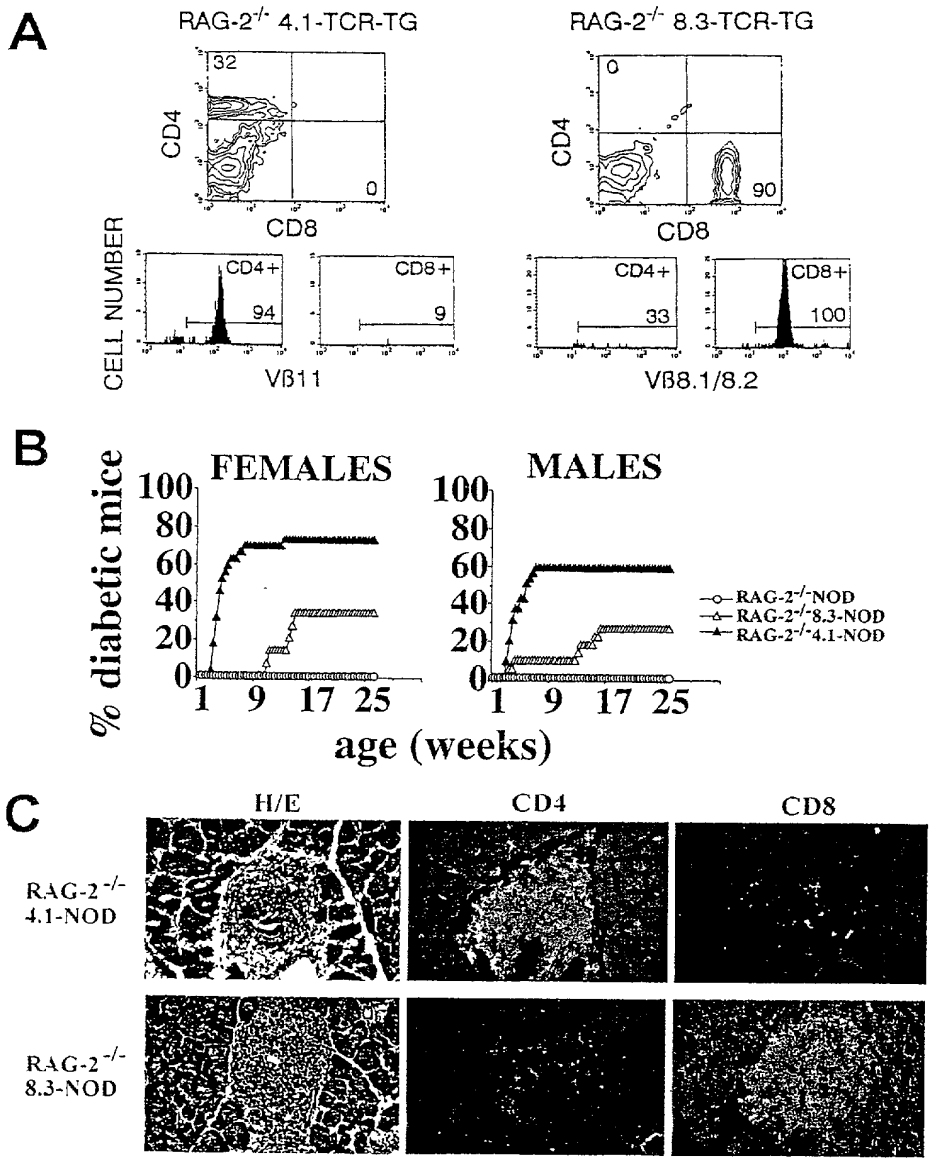

Fig. 4. Diabetogenesis in Monoclonal T-Cell NOD Mice. (A) FACS profiles of lymph node cells. (B) IDDM incidence. (C) Phenotype of insulitis T-cells. Most of the few CD8+ T-cells in RAG-2-/- 4.1-NOD mice, and the few CD4+ T-cells in RAG-2-/- 8.3-NOD mice are due to background staining, as they are also seen in anti-rat IgG-FITC-stained tissue.

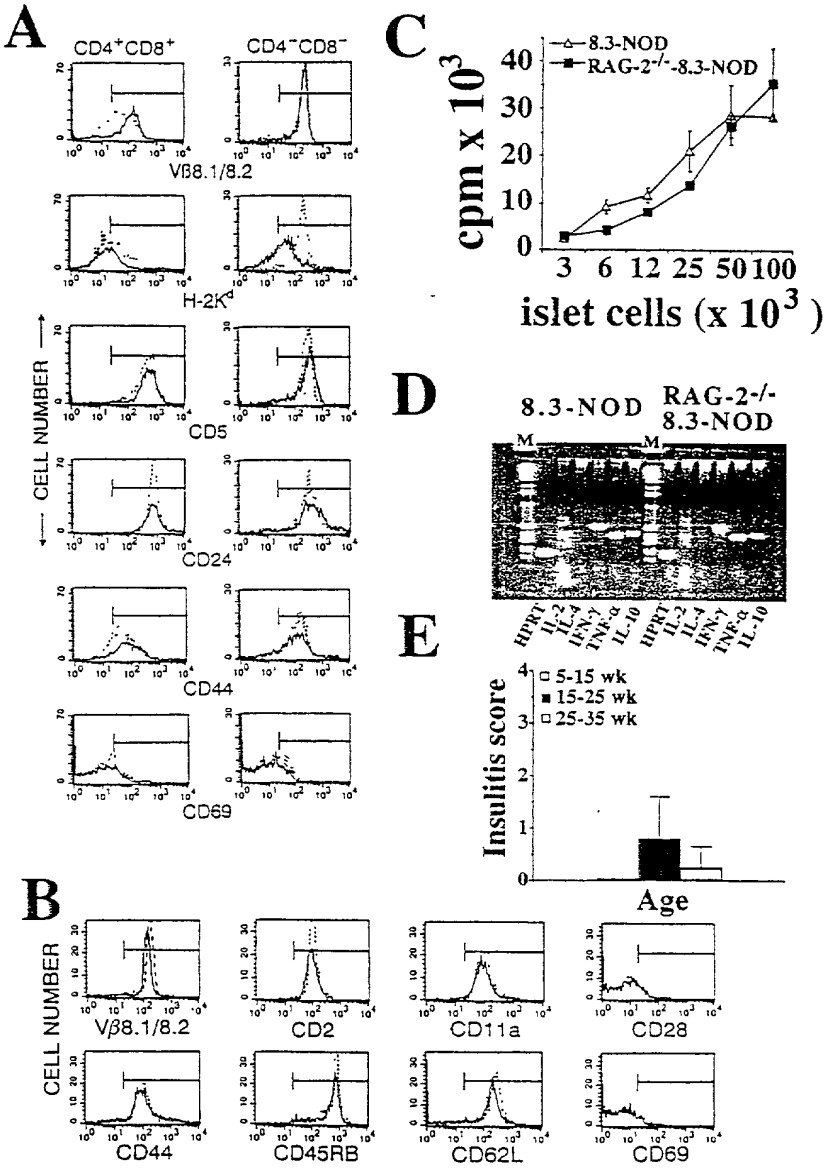

Fig. 5. Phenotypic and Functional Analysis of CD8+ T-cells from RAG-2⁻ 8.3-NOD Mice. **(A)** Maturation markers on thymocyte subsets from 8.3-NOD (dotted line) and RAG-2⁻ 8.3-NOD mice (solid line). **(B)** Activation/memory markers on splenic CD8⁺ T-cells from 8.3-NOD mice (dotted line) and RAG-2⁻ 8.3-NOD mice (solid line). **(C)** Proliferative activity of splenic CD8⁺ T-cells in response to islet cells. **(D)** Cytokine RT-PCR analysis of islet-derived CD8⁺ T-cells. **(E)** Kinetics of insulitis in RAG-2⁻ 8.3-NOD mice.

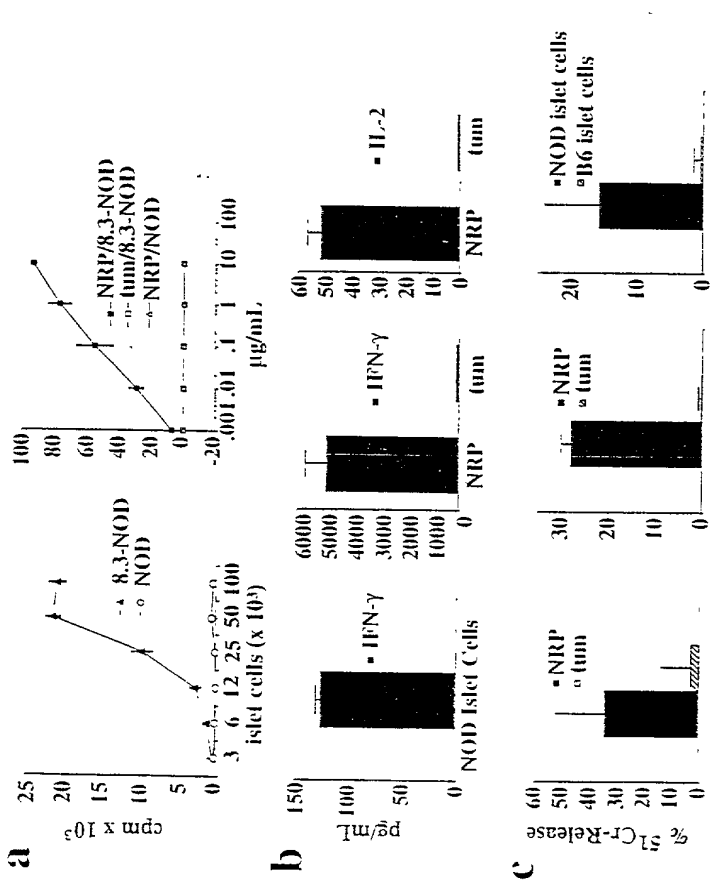

Fig. 6. Immunological Properties of NRP. A, Proliferation of CTLp from 8.3-NOD and NOD/Lt mice in response to NOD islet-cells (left) or NOD splenocytes pulsed with NRP or tum (right) ($p<0.05$ for islet cells or NRP- vs. tum-induced proliferation of 8.3-CTLp, and NRP-induced proliferation of 8.3-CTLp vs. NOD/Lt T-cells). **B,** Cytokine secretion by 8.3-CTLp in response to NOD islet cells or splenocytes pulsed with 1 μg/ml of NRP or tum (middle and right panels) ($p<0.009$ for IFN-γ/IL-2 secretion induced by NRP vs. tum). **C,** Differentiation of 8.3-CTLp from RAG-2$^{-/-}$ 8.3-NOD mice into CTL. The panel shows ^{51}Cr-release assays using NRP- or tum-pulsed RMA-Sᵏd cells (left and middle panels) or NOD or B6 islet cells as targets, at a 1:10 T:E ratio (right) ($p<0.05$ for NRP- vs. tum-reactivity or NOD- vs. B6 islet cell-reactivity).

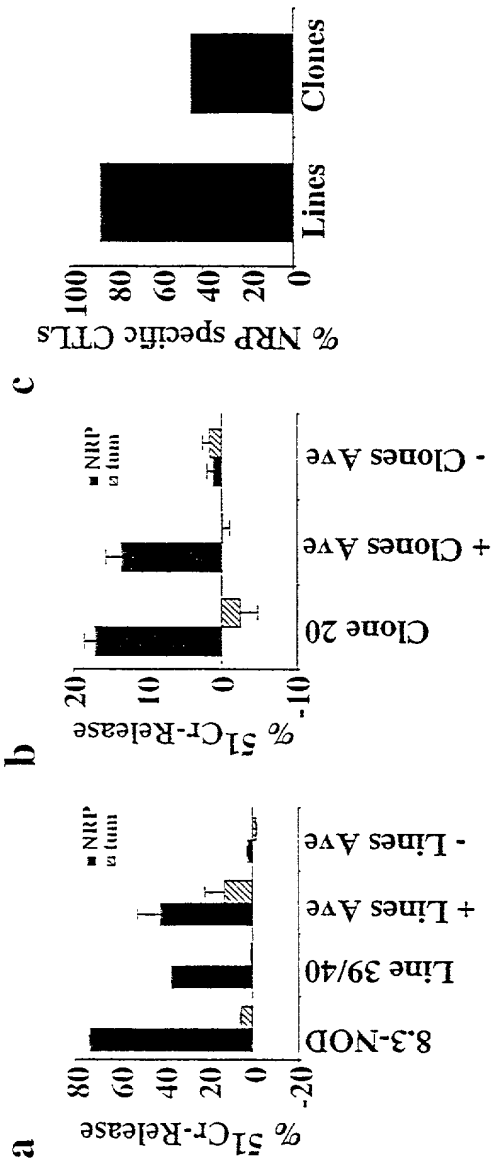

Fig. 7. NRP-reactivity of islet-associated $CD8^+$ T-cells from NOD/Lt mice. A, NRP- and tum-reactivity of islet- and spleen-derived $CD8^+$ T-cell lines from 8.3-NOD and/or NOD/Lt mice. CD3-act. are control CD8+ CTLs generated by stimulation of NOD splenic CD8+ T-cells with plate-bound anti-CD28 and anti-CD3 mAbs. The Fig. shows results of cytotoxicity assays obtained with 1 islet line, 2 splenic lines, and the average values obtained with 7 NRP-reactive and 1 non-reactive islet lines (at 1:10 T:E ratio) ($p<0.03$). The tum reactivity of the +Lines was due to one line which displayed some cytotoxicity against tum-pulsed targets. **B,** NRP-reactivity of islet-derived $CD8^+$ T-cell clones from NOD/Lt mice. Assays were done at a ≈1:1 T:E ratio. A clone was defined as positive if it triggered ^{51}Cr-release values from NRP-pulsed targets at least 2 SD above those triggered by tum-pulsed targets. The Fig. shows results of assays obtained with 1 clone, and average values corresponding to 14 NRP-reactive clones ($p<0.004$ for NRP- vs. tum-reactivity) and 17 non-NRP-reactive clones. **C,** % of NRP-reactive CTL lines and clones from NOD/Lt mice ($p<0.0001$ for % of NRP- vs. tum-reactive clones).

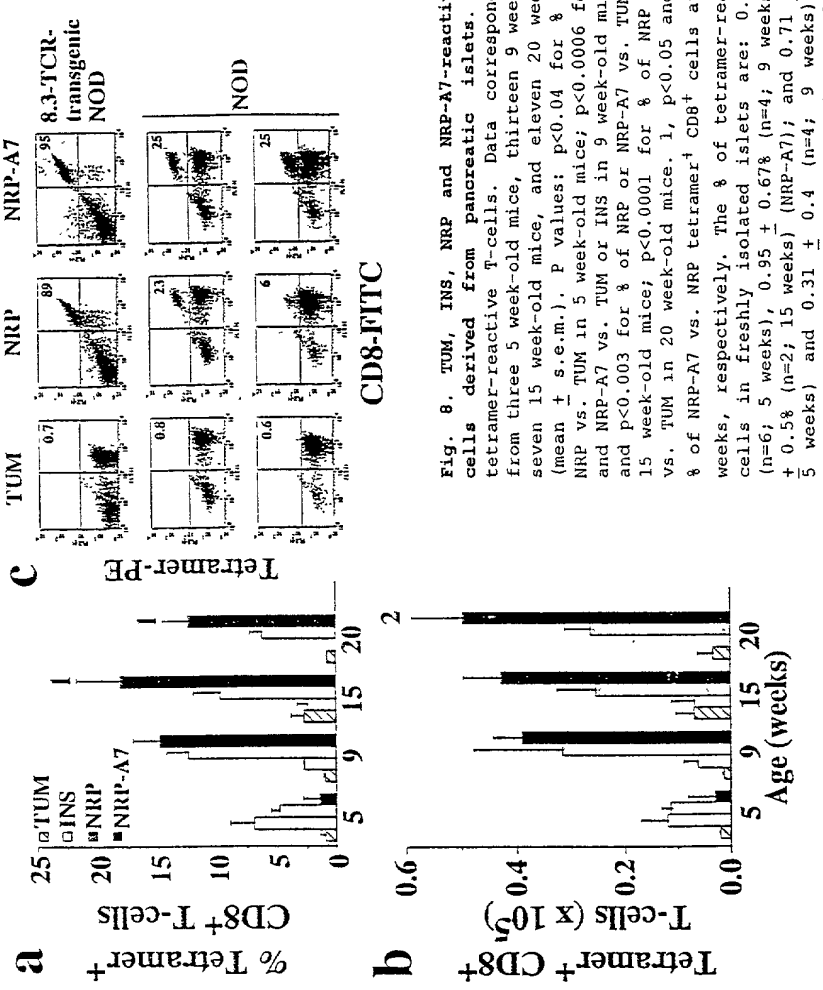

Fig. 8. TUM, INS, NRP and NRP-A7-reactive CD8⁺ T-cells derived from pancreatic islets. A, % of tetramer-reactive T-cells. Data correspond to cells from three 5 week-old mice, thirteen 9 week-old mice, seven 15 week-old mice, and eleven 20 week-old mice (mean ± s.e.m.). P values: $p<0.04$ for % of INS and NRP vs. TUM in 5 week-old mice; $p<0.0006$ for % of NRP and NRP-A7 vs. TUM or INS in 9 week-old mice; $p<0.013$ and $p<0.003$ for % of NRP or NRP-A7 vs. TUM or INS in 15 week-old mice; $p<0.0001$ for % of NRP and NRP-A7 vs. TUM in 20 week-old mice. 1, $p<0.05$ and 0.008 for % of NRP-A7 vs. NRP tetramer⁺ CD8⁺ cells at 15 and 20 weeks, respectively. The % of tetramer-reactive CD8⁺ cells in freshly isolated islets are: 0.13 ± 0.38% (n=6; 5 weeks), 0.95 ± 0.67% (n=4; 9 weeks), and 1.6 ± 0.58% (n=2; 15 weeks) (NRP-A7); and 0.71 ± 0.4 (n=4; 5 weeks) and 0.31 ± 0.4 (n=4; 9 weeks) (INS). **B,** Absolute number of tetramer-reactive T-cells from the same samples as in a (mean ± s.e.m.). P values: $p<0.04$ for NRP-A7 at 15 and 20 weeks vs. 9 and 5 weeks; $p<0.001$ for NRP and NRP-A7 vs. TUM at 9 weeks; $p<0.035$ for NRP or NRP-A7 vs. INS at 9 weeks; $p<0.037$ for NRP or NRP-A7 vs. TUM or INS at 15 weeks; $p<0.0001$ for NRP or NRP-A7 vs. TUM at 20 weeks. 2, $p<0.05$ NRP-A7 vs. NRP at 20 weeks. **C,** Representative tetramer staining patterns. Over 90% of the CD8-negative cells shown in the plots are $CD4^+$.

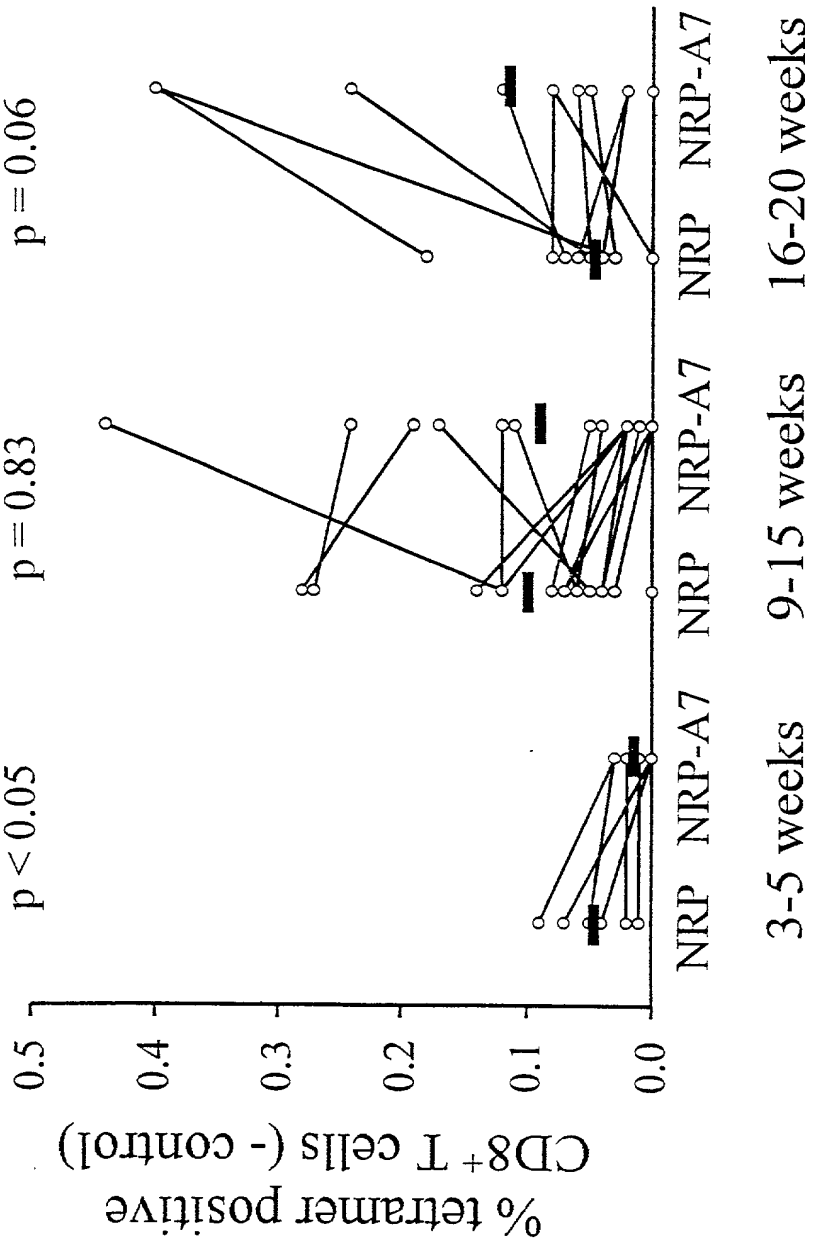

Fig. 9. Percentage of tetramer-positive CD8+ T-cells in pancreatic lymph nodes of NOD mice (data from J. Trudeau and R. Tan).

A

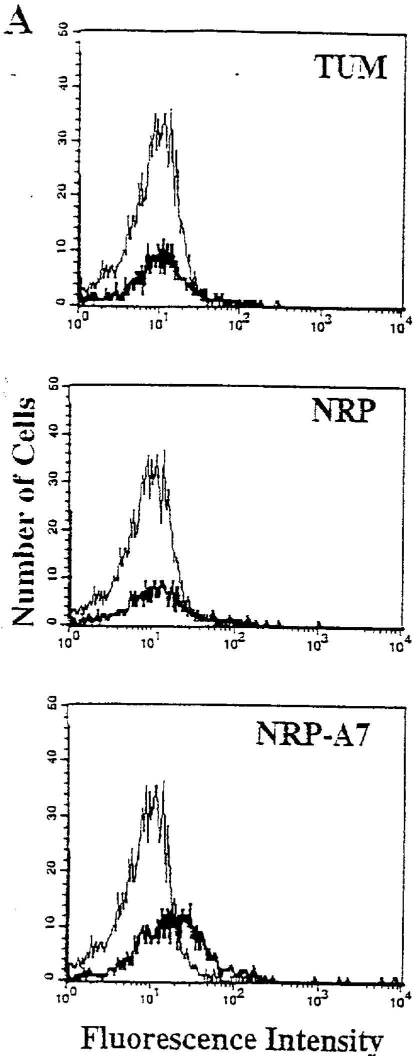

B

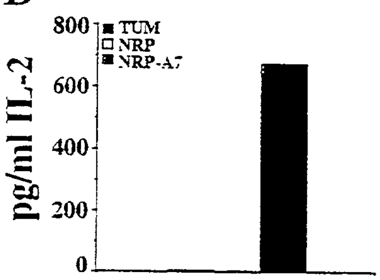

C

NY8.3	Vα17-Jα42	CA	MRD	SGGSNA
	Vβ8.1-Jβ2.4	CASS	D	AQNTLY
AI12-B1.3	Vα17-Jα42	CA	MRD	SGGSNA
	Vβ8.3-Jβ2.6	CASS	GDR	YEQYFG

Fig. 10. Some NRP-A7-reactive TCRs do not recognize NRP. A, reactivity of AI12-B1.3 TCR-transfected cells with TUM, NRP and NRP-A7-tetramers. B, secretion of IL-2 by the transfectant in response to stimulation with TUM, NRP and NRP-A7 peptides. C, TCR rearrangements of AI12-B1.3 (NRP-A7-reactive) and 8.3-CD8+ T-cells (NRP/NRP-A7-reactive). The TCR-alpha chains of these two clonotypes use different Vα17 family members (17.5 and 17.4, respectively).

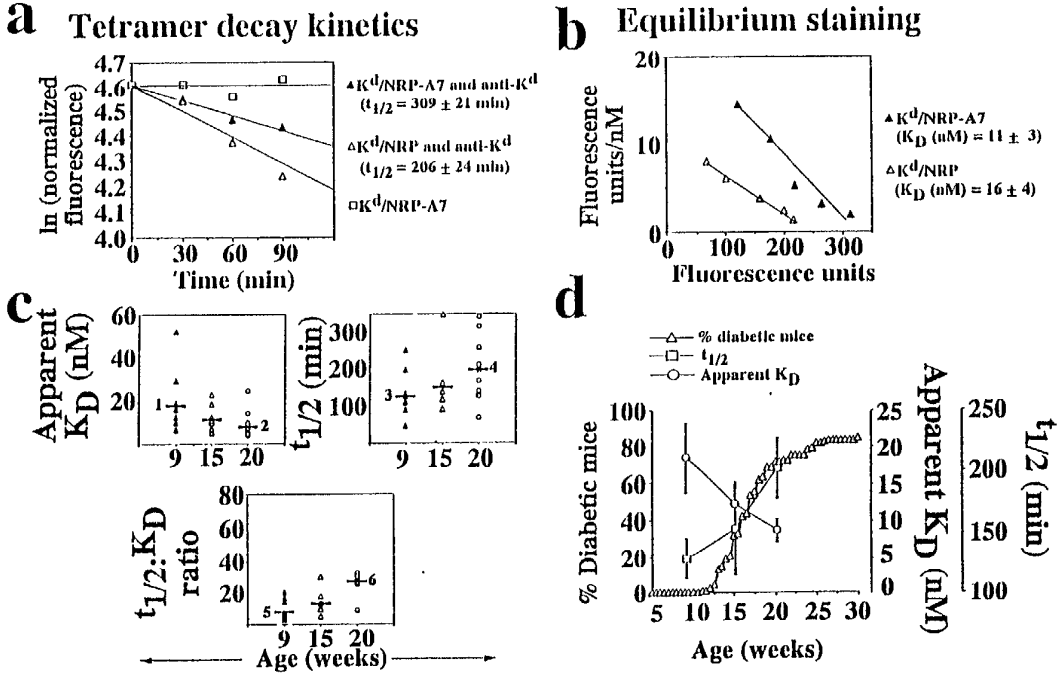

Fig. 11. Association and dissociation kinetics of NRP and NRP-A7 tetramers. A, Tetramer decay kinetics of 8.3-TCRαβ-transgenic $CD8^+$ T-cells (n=3). B, Scatchard analysis of tetramer binding to 8.3-TCRαβ-transgenic $CD8^+$ T-cells (n=3). Cells were stained with different concentrations of NRP and NRP-A7 tetramers and the fluorescence units/nM (bound tetramer/free tetramer) plotted against fluorescence units (bound tetramer). At the same concentration, the NRP tetramer occupies fewer T-cell receptors on 8.3-$CD8^+$ T-cells (FU) than the NRP-A7 tetramer. C, NRP-A7 tetramer association and dissociation kinetics for islet-derived $CD8^+$ T-cells from pre-diabetic NOD mice (n=9, 7 and 13 for K_D; n=11, 7 and 12 for $t_{1/2}$; and n=8, 7 and 12 for K_D:$t_{1/2}$ ratios at 9, 15 and 20 week-old time points, respectively). P values for cells from 9 vs. 20 week-old mice: K_D, $p<0.026$ (1 vs. 2); $t_{1/2}$, $p<0.027$ (3 vs. 4); $t_{1/2}$:K_D ratio, $p<0.015$ (5 vs. 6). The correlation coefficients for the average decay slopes (regression from 0-90 minutes) of samples from 9, 15 and 20 week-old mice were: 0.907 ($p<0.048$); 0.902 ($p=0.054$); 0.993 ($p<0.004$). There were statistical significant differences for the average of the ln of the normalized fluorescence at 90 minutes between the 9 and 20 week age groups (4.03 ± 0.08 vs. 4.29 ± 0.08, $p<0.013$). D, "avidity maturation" of NRP-A7-reactive cells (mean ± s.e.m.) vs. diabetes penetrance.

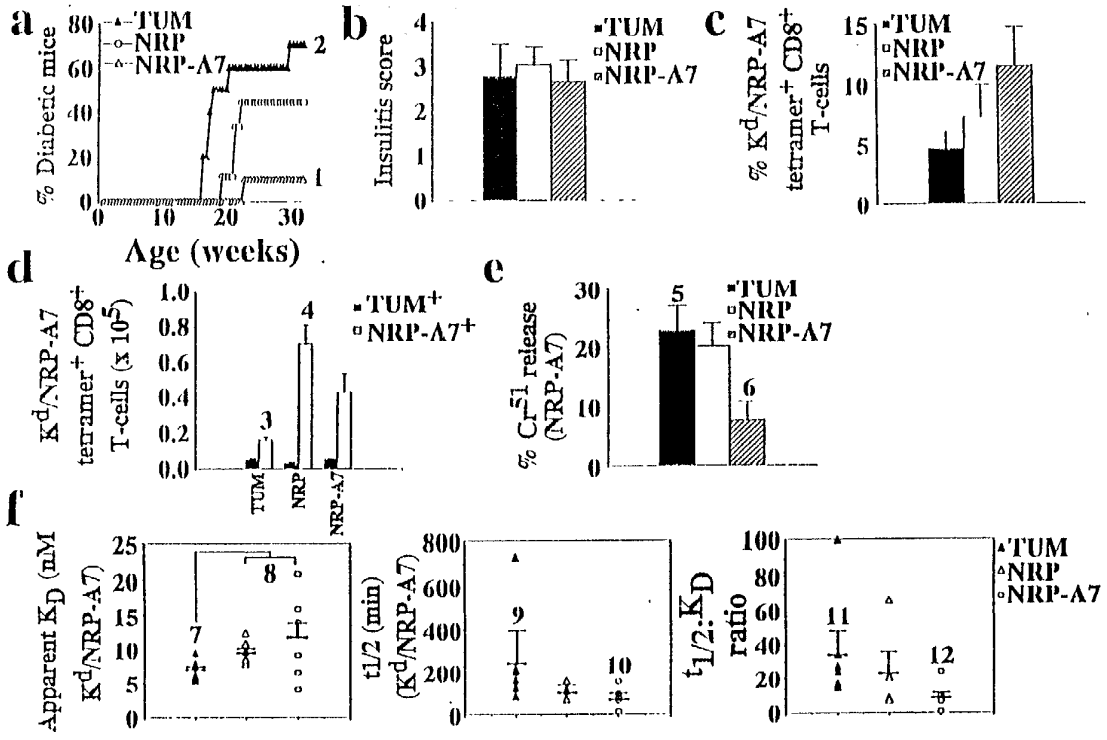

Fig. 12. Diabetogenesis in peptide-treated NOD mice. **A**, Incidence of diabetes in groups of 10 female NOD mice treated with intraperitoneal injections of TUM, NRP and NRP-A7 peptides in PBS. 1 vs. 2, $p<0.007$. **B**, Insulitis scores in non-diabetic mice (n=2-3 mice per group; mean ± s.e.m.). **C**, Percentage and **D**, Absolute number of NRP-A7 tetramer-reactive $CD8^+$ cells in peptide-treated mice (ip and fp routes; n=8 NRP-A7-, 9 NRP- and 10 control peptide-treated mice). 3 vs. 4, $p<0.015$. The percentage and number of $CD8^+$ cells isolated from peptide-treated mice were: 74 ± 3% and 4 ± 0.2 x 10^5 (TUM); 90 ± 1% and 5.7 ± 1 x 10^5 (NRP); and 86 ± 3% and 5.3 ± 0.9 x 10^5 (NRP-A7) ($p<0.03$ for NRP- plus NRP-A7-treated vs. control peptide-treated mice). No differences between diabetic and non-diabetic mice were observed. **E**, NRP-A7-specific minus TUM-specific cytotoxicity of $CD8^+$ T-cells from peptide-treated mice (ip and fp routes; n=7 NRP-A7-, 11 NRP- and 13 control peptide-treated mice (mean ± s.e.m.). No differences between diabetic and non-diabetic mice were noted. $p<0.017$ for 5 vs. 6. **F**, NRP-A7 tetramer binding kinetics of $CD8^+$ T-cells from non-diabetic 32 wk-old peptide-treated mice (ip and fp routes; n=5 NRP-A7-, 4 NRP- and 6 control peptide-treated mice) (mean ± s.e.m.). P values: 7 vs. 8, $p<0.05$; 9 vs. 10, $p<0.04$; 11 vs. 12, $p<0.02$. The correlation coefficients for the average decay slopes (0-90 minutes) of samples from control peptide-, NRP- and NRP-A7-treated mice were: 0.954 ($p<0.023$); 0.899 ($p=0.054$); 0.979 ($p<0.03$). The ln (normalized fluorescence) values at 90 minutes between the control peptide- and NRP-A7-treated groups were 3.88 ± 0.12 vs. 4.31 ± 0.15 ($p=0.055$).

APPLN. FILING DATE: HEREWITH
TITLE: COMPOSITIONS AND METHODS USEFUL IN AVIDITY...
INVENTOR(S): PERE SANTAMARIE
APPLICATION SERIAL NO: NEW

Figure 13

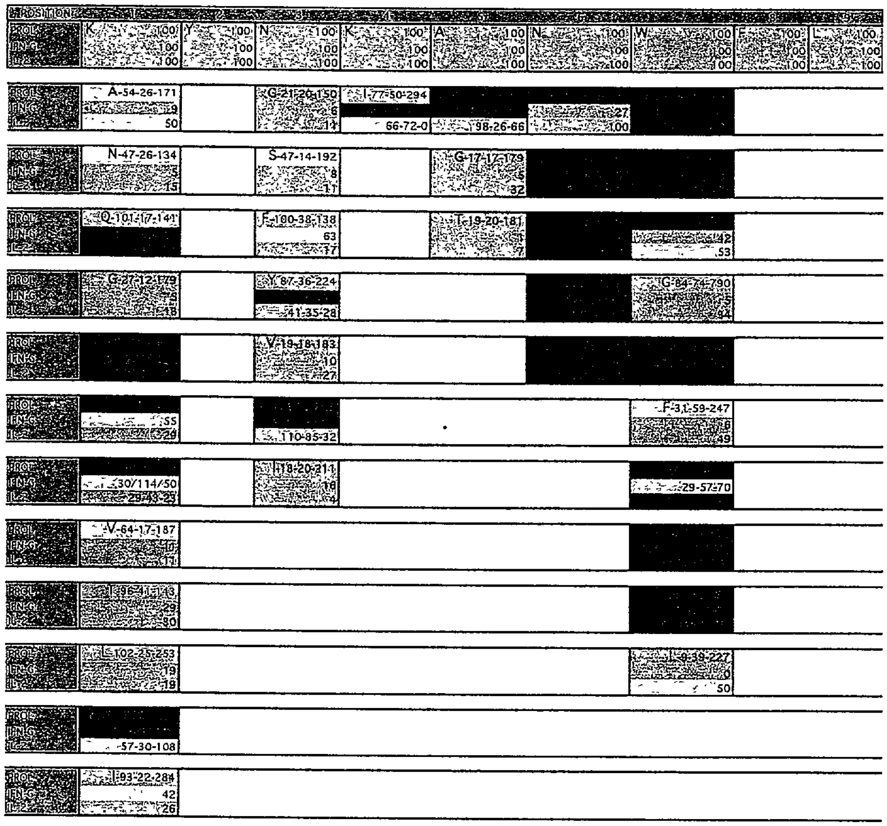
A-54-26-171
N-47-26-134
S-47-14-192
66-72-0
98-26-66
30/114/50
29-57-70
F-31-59-247
110-85-32
V-64-17-187
-57-30-108

Figure 14

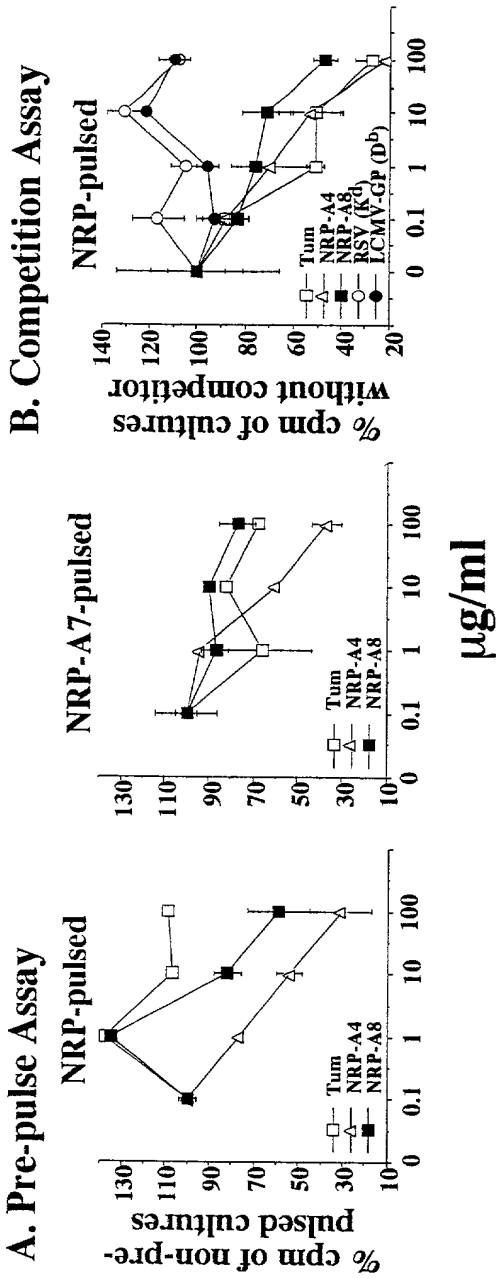
A. Pre-pulse Assay
NRP-pulsed
% cpm of non-pre-pulsed cultures
Tum
NRP-A4
NRP-A8
NRP-A7-pulsed
B. Competition Assay
NRP-pulsed
% cpm of cultures without competitor
RSV (Kd)
LCMV-GP (Db)
µg/ml

FIGURE 15

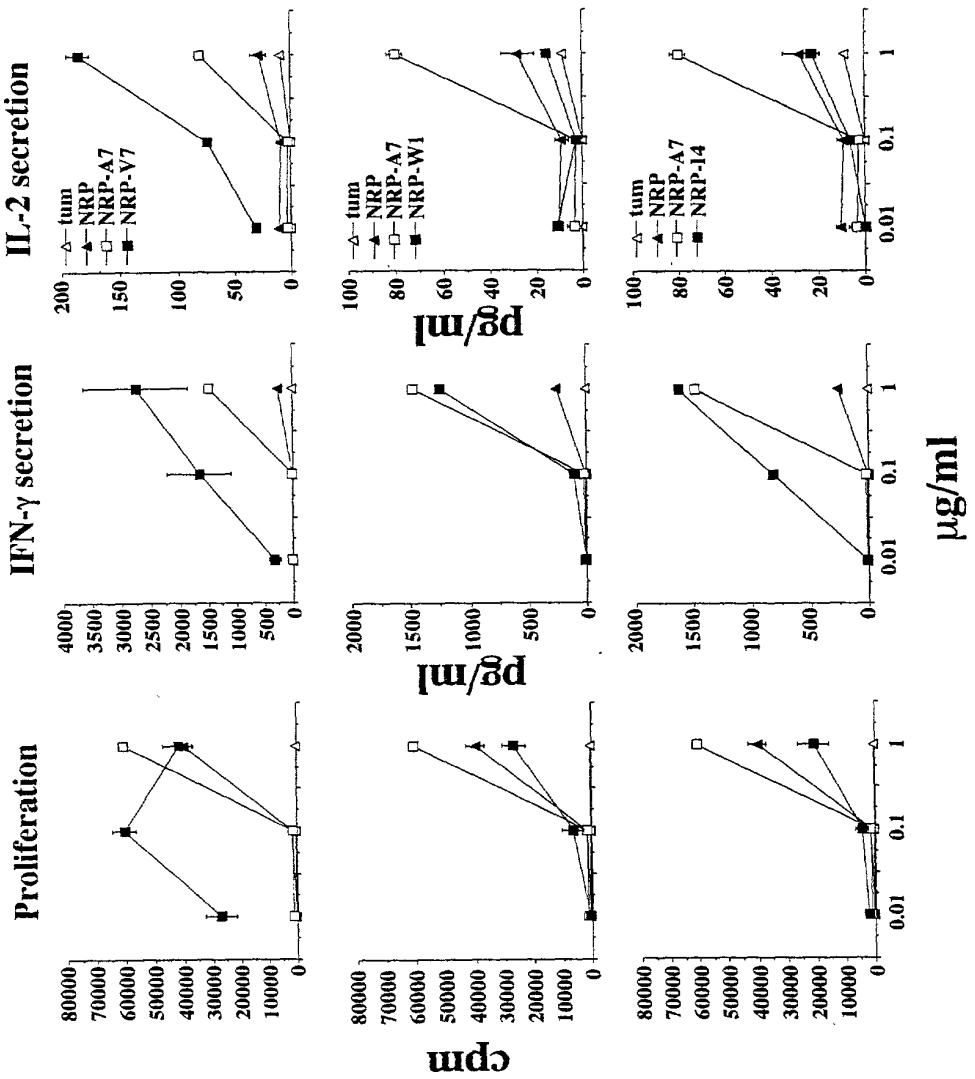
IL-2 secretion
IFN-γ secretion
Proliferation
tum
NRP
NRP-A7
NRP-V7
NRP-W1
NRP-14
pg/ml
cpm
μg/ml

FIGURE 16

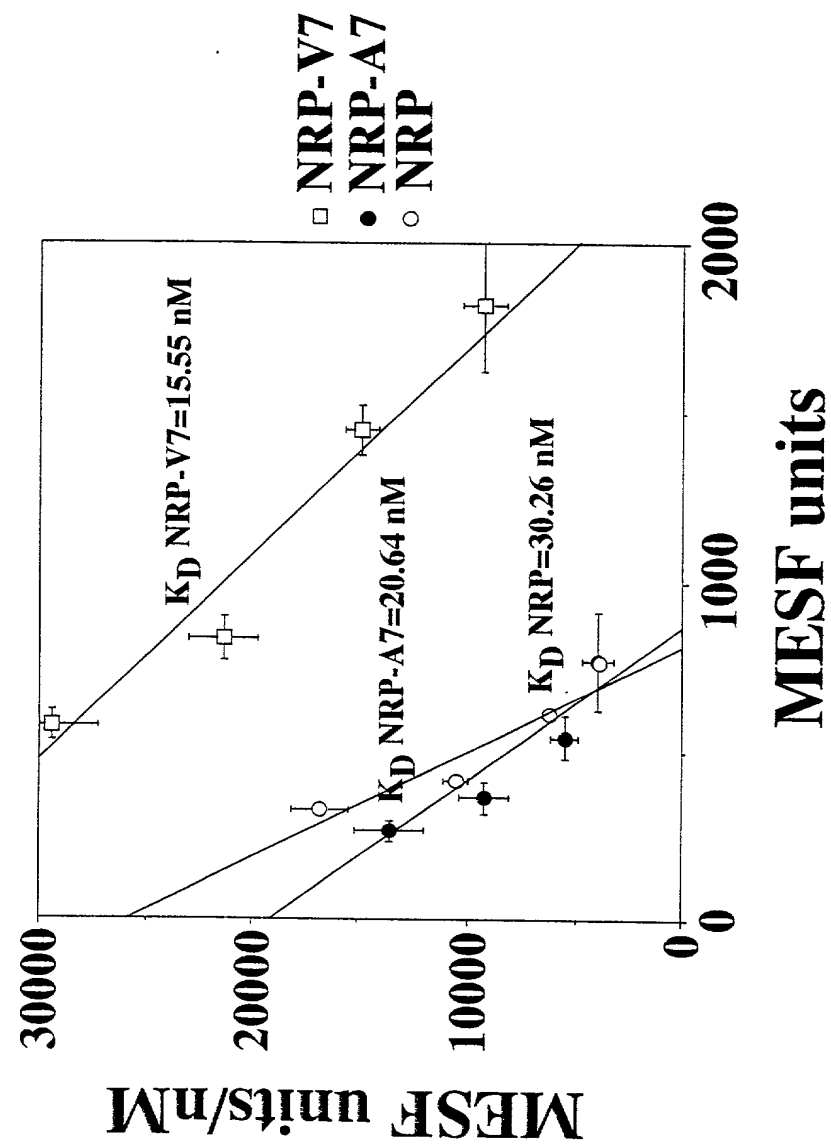
NRP-V7
NRP-A7
NRP
K_D NRP-V7=15.55 nM
K_D NRP-A7=20.64 nM
K_D NRP=30.26 nM
MESF units/nM
30000
20000
10000
0
0
1000
2000
MESF units

FIGURE 17

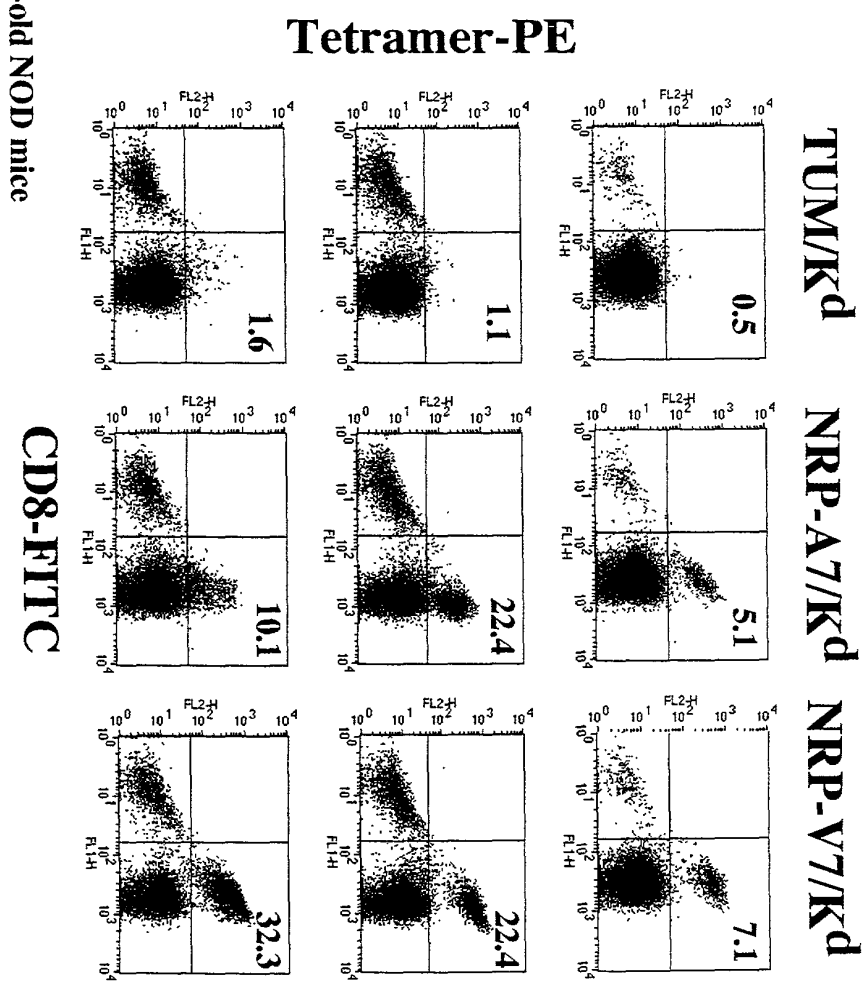
Tetramer-PE
TUM/Kd
NRP-A7/Kd
NRP-V7/Kd
CD8-FITC
20 week-old NOD mice
1.6
1.1
0.5
10.1
22.4
5.1
32.3
22.4
7.1
FL2-H
FL1-H

FIGURE 18

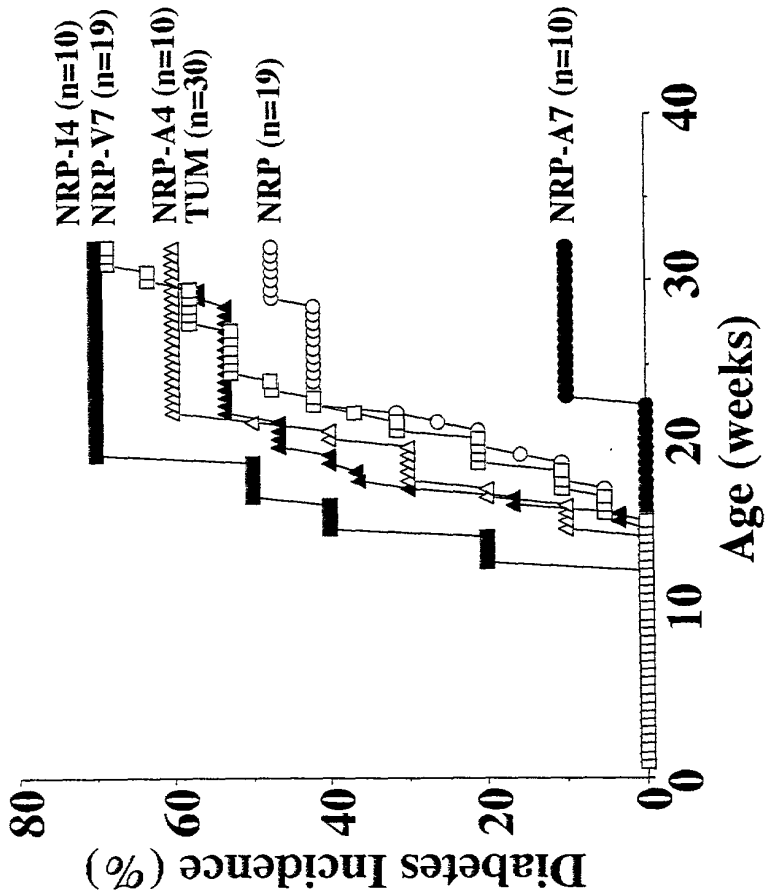
NRP-I4 (n=10)
NRP-V7 (n=19)
NRP-A4 (n=10)
TUM (n=30)
NRP (n=19)
NRP-A7 (n=10)
Diabetes Incidence (%)
0
20
40
60
80
0
10
20
30
40
Age (weeks)

FIGURE 19

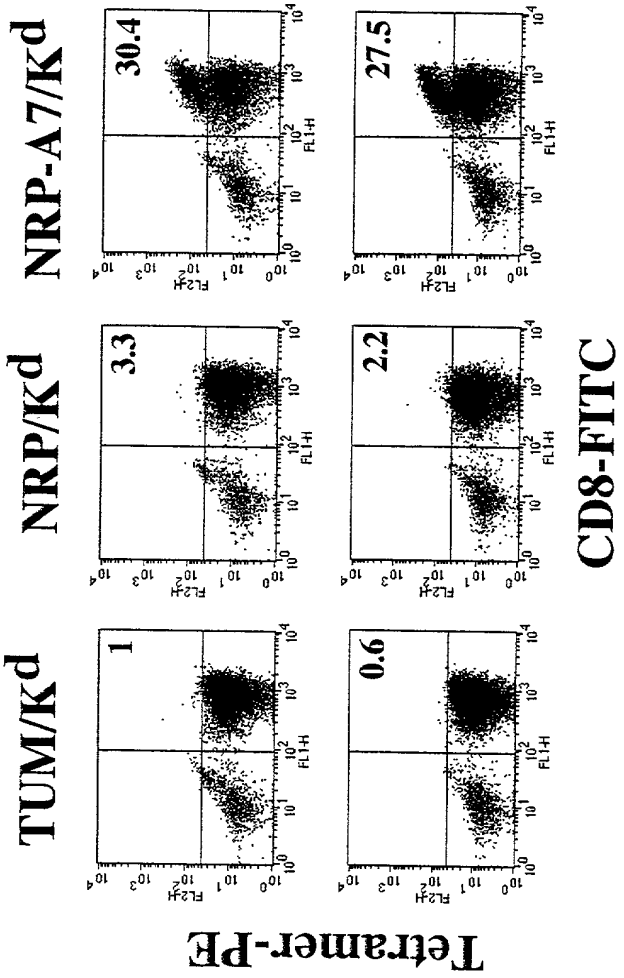
NRP-A7/K^d
NRP/K^d
TUM/K^d
30.4
27.5
3.3
2.2
1
0.6
Tetramer-PE
CD8-FITC
NRP-I4-treated NOD mice (@32 wk)

FIGURE 20

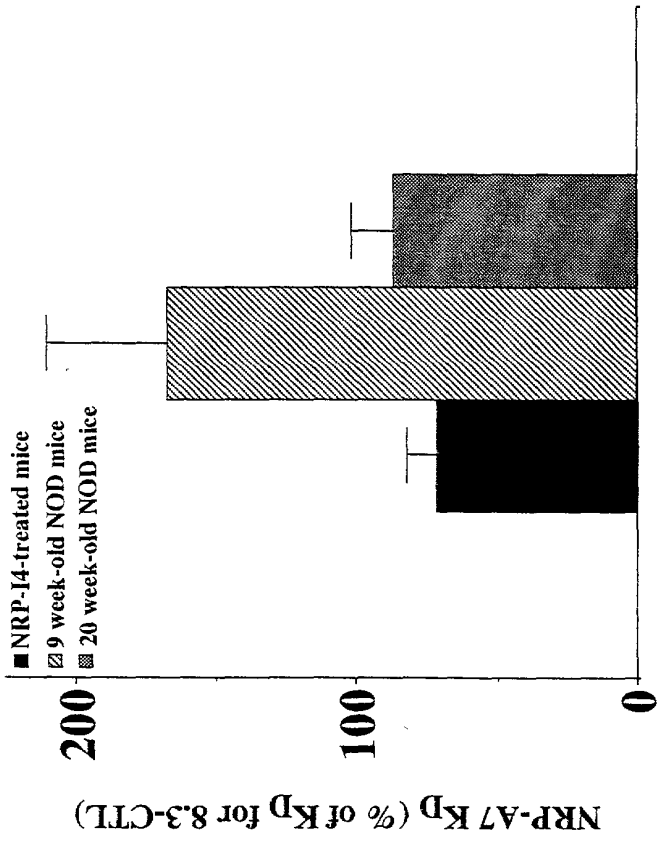
NRP-A7 KD (% of KD for 8.3-CTL)
200
100
0
NRP-I4-treated mice
9 week-old NOD mice
20 week-old NOD mice

FIGURE 21

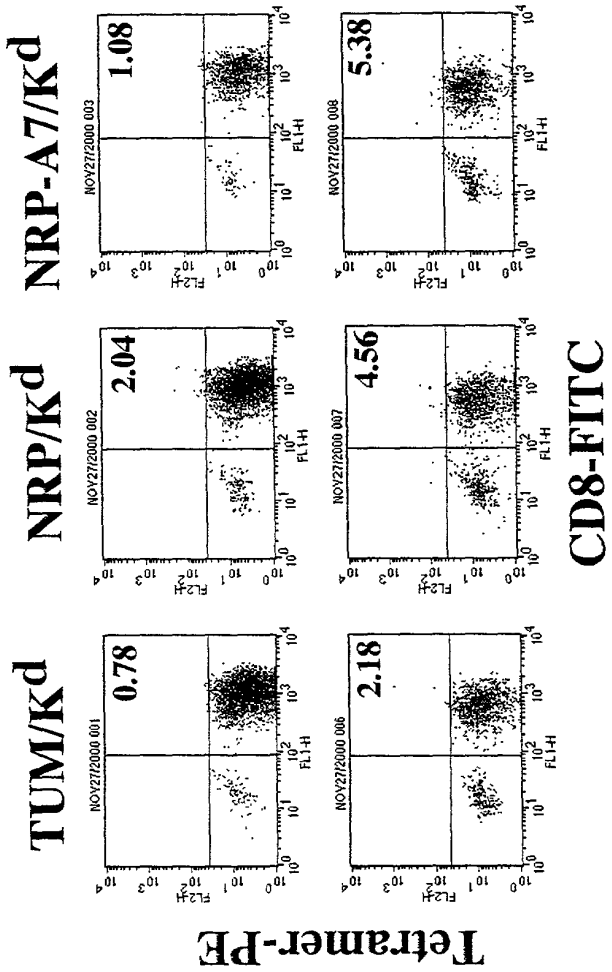
NRP-A7/Kd
NRP/Kd
TUM/Kd
1.08
5.38
2.04
4.56
0.78
2.18
NOV27/2000 003
NOV27/2000 008
NOV27/2000 002
NOV27/2000 007
NOV27/2000 001
NOV27/2000 006
FL1-H
FL2-H
CD8-FITC
Tetramer-PE

FIGURE 22

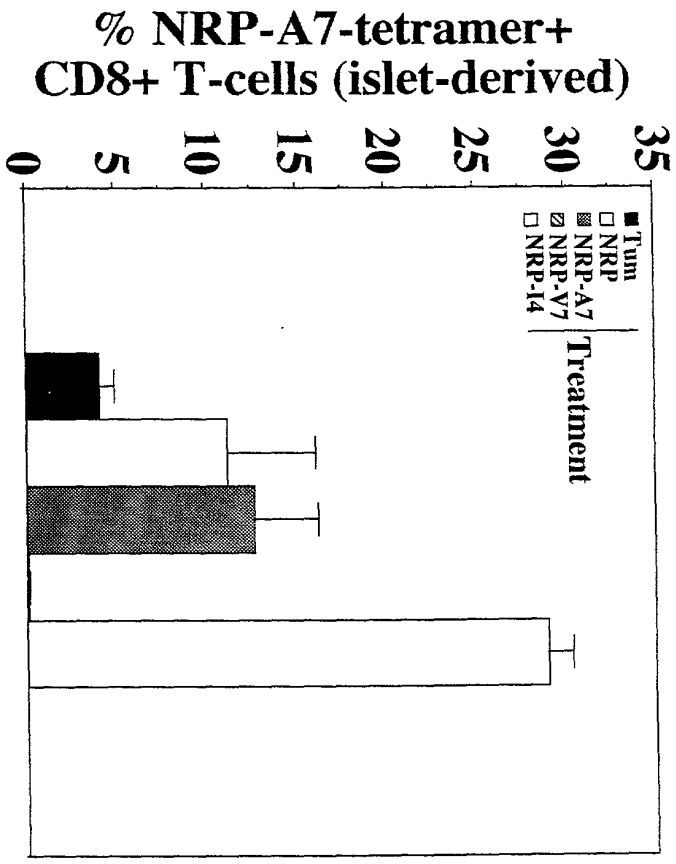

FIGURE 23

high affinity T-cell
low affinity T-cell
too strong an interaction => deletion
still too strong an interaction => deletion
BAD OUTCOME: DELETES A DOMINANT T-CELL POPULATION AND CREATES A NICHE
super-superagonist
too strong an interaction => deletion
moderate interaction => activation
GOOD OUTCOME: DELETES THE MOST PATHOGENIC T-CELLS AND LEADS TO AN EXPANSION OF NON-PATHOGENIC AUTOREACTIVE T CELLS THAT OCCUPY THE NICHE
superagonist
strong an interaction => activation/deletion
moderate interaction => weak activation
NEITHER GOOD NOR BAD: THE BALANCE REMAINS THE SAME
agonist
weak interaction => activation
too weak an interaction => no activation/no deletion
TERRIBLE OUTCOME: SELECTIVE EXPANSION OF PATHOGENIC T-CELLS
partial agonist

FIGURE 24

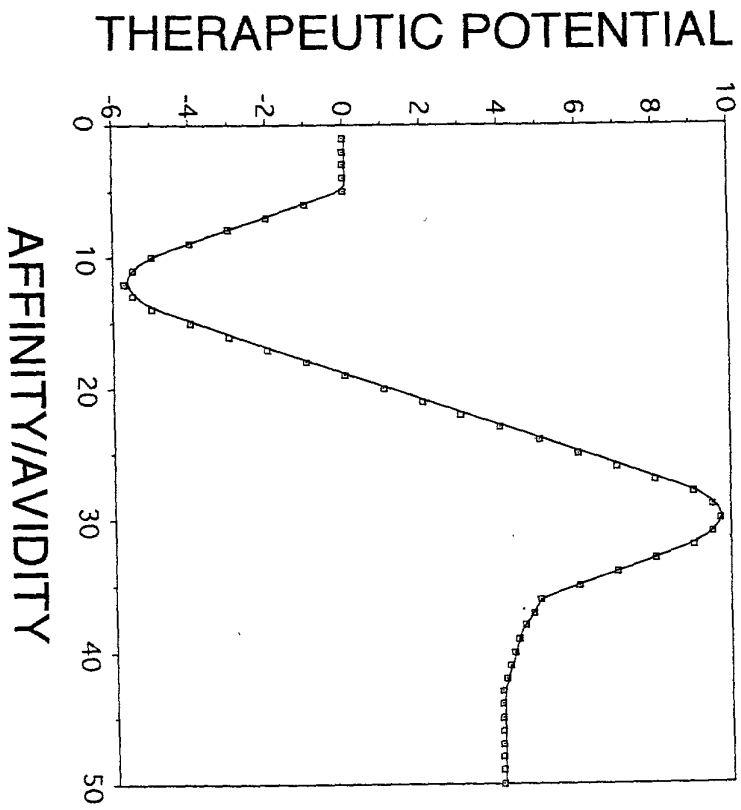

Low affinity NRP mimics and Type 1 Diabetes (T1D)

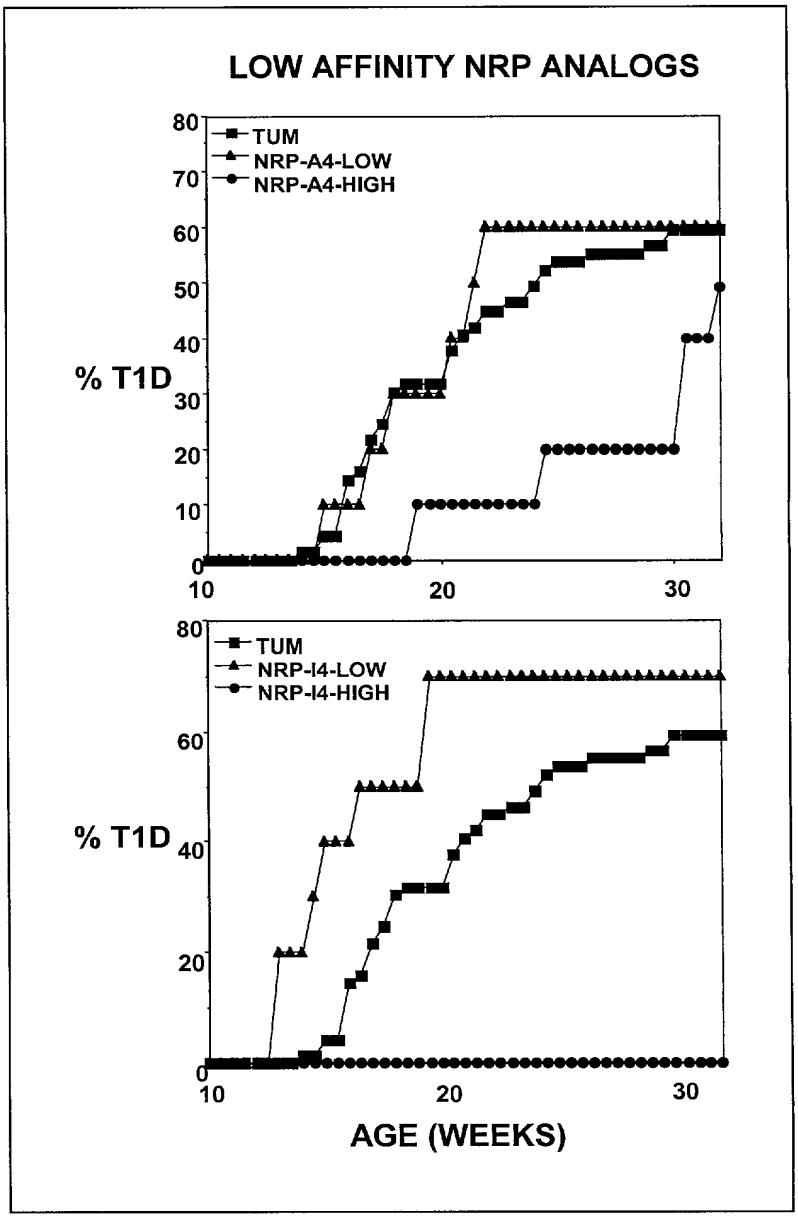

High affinity NRP mimics and Type 1 Diabetes (T1D)

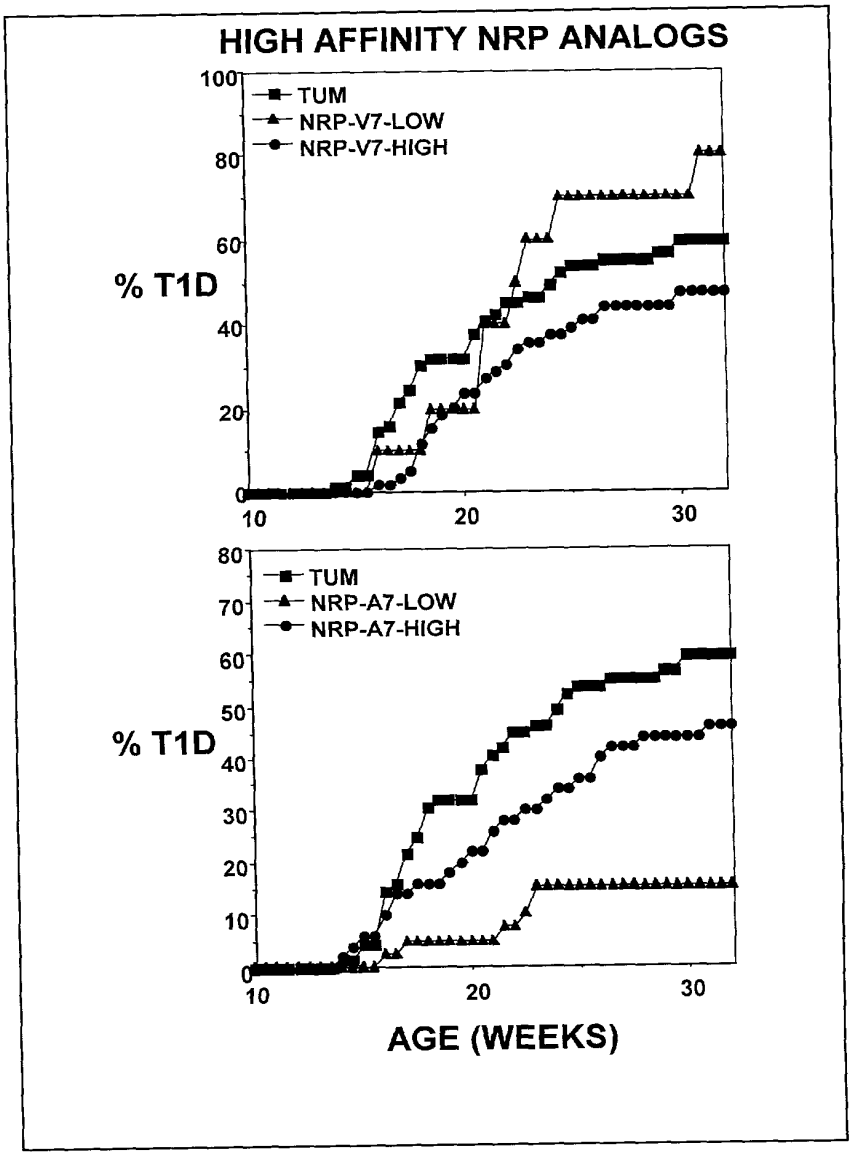

Anti-diabetogenic regimens and expansion of low avidity cells in islets

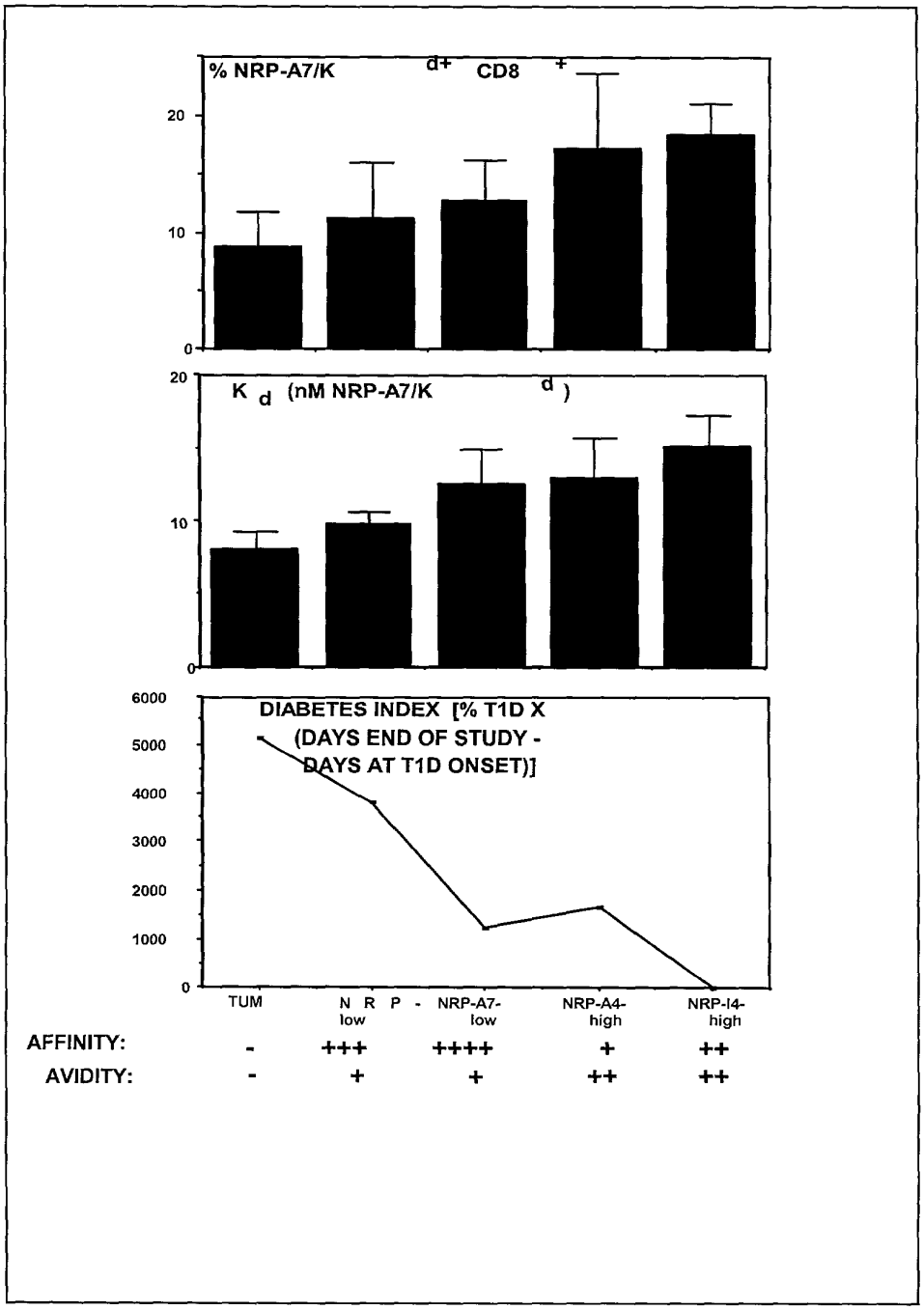

Expansion of "irrelevant" autoreactive cells by elimination of other specificities